Journal for ImmunoTherapy of Cancer

Targeting PD-1 and CD85j can restore intratumoral CD4$^+$ GzmB$^+$ T-cell functions to combat MHC-II-expressing tumors

Boyu Wang, Xu Wang, Tianlai Wang, Kelin Meng, Taiyan Yu, Yu Xi, Shaojie Hu, Hui Xiong, Rirong Qu, Zhiwei Yuan, Xue Wang, Chenxi Zeng, Wenbin Zou, Yitao Tian, Yixin Cai, Shengling Fu, Xiangning Fu, Lequn Li

To cite: Wang B, Wang X, Wang T, *et al*. Targeting PD-1 and CD85j can restore intratumoral CD4$^+$ GzmB$^+$ T-cell functions to combat MHC-II-expressing tumors. *Journal for ImmunoTherapy of Cancer* 2025;**13**:e010890. doi:10.1136/jitc-2024-010890

► Additional supplemental material is published online only. To view, please visit the journal online (https://doi.org/10.1136/jitc-2024-010890).

Accepted 16 March 2025

Department of Thoracic Surgery, Huazhong University of Science and Technology Tongji Medical College Tongji Hospital, Wuhan, Hubei, China

Correspondence to
Dr Lequn Li;
lqli@tjh.tjmu.edu.cn

Professor Xiangning Fu;
fuxn2006@aliyun.com

ABSTRACT

Background A subset of CD4$^+$ T cells with cytotoxic activity has been identified, and these cells exert their effects by expressing perforin and granzymes. Despite the progress made in characterizing cytotoxic CD4$^+$ T cells in various diseases, the status of cytotoxic CD4$^+$ T cells in non-small cell lung cancer (NSCLC) and the underlying mechanisms involved in promoting intratumoral cytotoxic CD4$^+$ T-cell activation remain unclear.

Methods We used flow cytometry to examine the phenotypic and functional properties of CD4$^+$GzmB$^+$ T cells in the peripheral blood and tumor tissues of patients with NSCLC. Loss-of-function analyses and RNA sequencing were used to identify the underlying mechanisms involved in the effects of interleukin (IL)-15 on the restoration of CD4$^+$GzmB$^+$ T-cell function in vitro. A patient-derived lung cancer explant model and an animal model were used to verify the effects of immune checkpoint inhibitors on CD4$^+$GzmB$^+$ T-cell activation.

Results In patients with NSCLC, impaired cytolytic function of tumor-infiltrated granzyme B (GzmB)-expressing CD4$^+$ T cells was restored by IL-15 through activation of the AKT-FOXO1-T-bet axis. Moreover, IL-15 stimulation increased solute carrier family 7 member 5 (SLC7A5) expression in CD4$^+$GzmB$^+$ T cells in an Protein Kinase B (AKT)-dependent manner, and inhibition of SLC7A5 abrogated the effect of IL-15 on CD4$^+$GzmB$^+$ T cells. Additionally, we showed that the immune checkpoint molecules programmed cell death-1 (PD-1) and CD85j were mutually exclusively expressed in CD4$^+$GzmB$^+$ T cells and that dual targeting of PD-1 and CD85j enhanced the effector function of CD4$^+$GzmB$^+$ T cells by activating the AKT pathway. Notably, tumor cells expressing major histocompatibility complex (MHC)-II and IL-15 determine the effectiveness of CD4$^+$GzmB$^+$ T-cell-mediated antitumor immunity in response to immunotherapy.

Conclusions Our study demonstrated that tumor-infiltrating CD4$^+$GzmB$^+$ T cells fail to eliminate tumors. Dual blockade of PD-1 and CD85j alongside IL-15 restores the effector function of CD4$^+$GzmB$^+$ T cells and drives CD4$^+$GzmB$^+$ T-cell transformation in the tumor microenvironment to combat MHC-II-expressing tumors.

WHAT IS ALREADY KNOWN ON THIS TOPIC

⇒ Tumor-infiltrating CD4$^+$GzmB$^+$ cells are associated with immunotherapy efficacy.

⇒ The phenotypic and functional properties of intratumoral CD4$^+$GzmB$^+$ T cells have been reported. However, the underlying mechanisms and factors regulating intratumoral CD4$^+$GzmB$^+$ T-cell development and effector function remain unclear.

WHAT THIS STUDY ADDS

⇒ Interleukin (IL)-15 expression within tumors enhances the effector function of intratumoral CD4$^+$GzmB$^+$ T cells through activation of the AKT-FOXO1-T-bet axis.

⇒ Additionally, IL-15 stimulation increases solute carrier family 7 member 5 (SLC7A5) expression in CD4$^+$GzmB$^+$ T cells in an Protein Kinase B (AKT)-dependent manner, and the inhibition of SLC7A5 abrogates the effect of IL-15 on CD4$^+$GzmB$^+$ T cells.

⇒ Intratumoral CD4$^+$GzmB$^+$ T cells highly express programmed cell death-1 (PD-1) and CD85j. Importantly, PD-1 and CD85j are mutually exclusively expressed by intratumoral CD4$^+$GzmB$^+$ T cells. Dual blockade of PD-1 and CD85j synergistically increased the effector function of CD4$^+$GzmB$^+$ T cells.

⇒ The effectiveness of CD4$^+$GzmB$^+$ T-cell-mediated antitumor immunity in response to immunotherapy requires tumor cells expressing major histocompatibility complex (MHC)-II and IL-15.

HOW THIS STUDY MIGHT AFFECT RESEARCH, PRACTICE OR POLICY

⇒ This work provides new insights into the molecular mechanisms underlying the activation of CD4$^+$GzmB$^+$ T cells and identifies the critical factors that drive CD4$^+$GzmB$^+$ T-cell transformation in the tumor microenvironment to combat MHC-II-expressing non-small cell lung cancer.

BACKGROUND

Cytotoxic CD8$^+$ T cells have long been recognized as the most powerful effector cells in the anticancer immune

response; thus, most cancer immunotherapies focus on enhancing the antitumor cytotoxic CD8+ T-cell response.[1 2] Unlike cytotoxic CD8+ T cells, CD4+ T cells are highly versatile and represent heterogeneous subsets with specialized effector functions[3 4]; therefore, the contribution of CD4+ T cells to the efficacy of antitumor immunity and immunotherapy is not yet fully understood. As the use of single-cell RNA sequencing (RNA-seq) technology has increased, the importance of cytotoxic CD4+ T cells in antitumor immunity and immunotherapy has become apparent. A sophisticated study by Oh *et al* revealed that a gene signature of cytotoxic CD4+ T cells in tumors predicts the clinical response of patients with metastatic bladder cancer to anti-programmed death-ligand 1 (PD-L1) therapy.[5] Moreover, a very recent study reported that human cytotoxic CD4+ T cells can mediate tumor clearance independent of CD8+ T cells in a humanized immune system mouse model.[6]

Cytotoxic CD4+ T cells express perforin and contain high levels of granzymes. To date, most studies have demonstrated that cytotoxic CD4+ T cells directly kill target cells in a major histocompatibility complex (MHC)-II-restricted manner.[7 8] Single-cell transcriptomic analysis of cytotoxic CD4+ T cells in patients with metastatic renal cell carcinoma revealed that there are two distinct types of cytotoxic CD4+ T cells: CD4+GzmK+ T cells and CD4+GzmB+ T cells. Interestingly, trajectory analysis indicated that weakly cytotoxic CD4+GzmK+ T cells differentiated from their CD4+GzmB+ counterparts.[9] Moreover, analysis of T-cell receptors (TCRs) revealed that cytotoxic CD4+ T cells can accumulate through clonal expansion.[10 11] The T-box transcription factors T-bet and eomesodermin (Eomes) play essential roles in driving the differentiation of cytotoxic CD4+ T cells.[12 13] Additionally, RUNX family transcription factor 3 (Runx3), a key transcription factor for CD8+ T-cell development and cytotoxic activity, can be detected in cytotoxic CD4+ T cells.[14–16] However, our understanding of how these cells are generated and activated in the context of cancer immunity and immunotherapy remains very limited.

In this study, we examined the status of CD4+GzmB+ T cells in patients with non-small-cell lung cancer (NSCLC). We showed that the cytolytic activity of intratumoral CD4+GzmB+ T cells is impaired and can be significantly revived by interleukin (IL)-15 through activation of the AKT-FOXO1-T-bet pathway as well as by dual blockade of programmed cell death-1 (PD-1) and CD85j. Additionally, we showed that the generation and effector function of CD4+GzmB+ T cells require the induction of solute carrier family 7 member 5 (SLC7A5) expression. Moreover, intrinsic MHC-II expression in tumor cells determines the contribution of CD4+GzmB+ T-cell-mediated antitumor immunity to immunotherapy efficacy.

METHODS

Study participants and sample collection

Peripheral blood samples and tumor specimens were collected from 71 patients who were diagnosed with NSCLC and underwent pulmonary resection between October 2021 and October 2024 in the Department of Thoracic Surgery at Tongji Hospital. Peripheral blood samples were obtained before primary tumor resection. Primary tumor and peritumoral normal lung tissues were obtained during surgery. Tumor, node, metastases (TNM) stage was determined according to the 2017 American Joint Committee on Cancer staging guidelines (eighth edition of the TNM classification). Patients who had been previously treated with radiation, chemotherapy or immunotherapy before surgery or who had autoimmune disease or infectious diseases were excluded. This study was performed under the tenets of the Declaration of Helsinki. The clinicopathological characteristics of the enrolled patients with NSCLC are shown in online supplemental table S1.

Antibodies and reagents

All the antibodies and reagents used are listed in online supplemental table S2.

Purification of CD4+ T cells

CD4+ T cells were purified via positive selection with human/mouse CD4 MicroBeads according to the manufacturer's instructions (Miltenyi Biotec, Germany). The purity of the CD4+ T cells was greater than 95%.

Stimulation of T cells

To assess interferon (IFN)-γ production by CD4+ T cells ex vivo, lymphocytes (5×10^5 cells/well, 96-well plate) were cultured in the presence or absence of 50 ng/mL phorbol-12-myristate-13-acetate (Sigma Aldrich, St. Louis, Missouri, USA) plus 250 ng/mL ionomycin (EMD Millipore, Billerica, Massachusetts, USA) for 4 hours. Monensin (BD Biosciences, San Jose, California, USA) was added for intracellular IFN-γ staining. Alternatively, lymphocytes (1×10^5 cells/well, 96-well plate) from peripheral blood mononuclear cells (PBMCs) and tumor-infiltrating lymphocytes (TILs) were treated with 1 µg/mL CD3 monoclonal antibody (mAb) plus 0.5 µg/mL CD28 mAb in the presence or absence of IL-15 (10 ng/mL).

Flow cytometry

For intracellular staining, PBMCs or TILs (1×10^6 cells/sample) were first stained with cell surface markers with the indicated antibodies and then fixed and permeabilized via a FoxP3/Transcription Factor Staining Buffer Kit (eBioscience). For phosphorylated protein and SLC7A5 staining, PBMCs or TILs (1×10^6 cells/sample) were stained with antibodies against cell surface markers on ice for 30 min, fixed with BD Cytofix Buffer and permeabilized on ice for 30 min with BD Phosflow Perm Buffer. Information on the antibodies used for surface and

intracellular staining is provided in online supplemental table S2.

Flow cytometric analysis was performed on an Attune NxT (Thermo Fisher Scientific, Wyman Street, Waltham, Massachusetts, USA). Dead cells were excluded by using Fixable Viability Dye eFluo 780 (eBioscience). The cell clumps and doublets were removed by pulse area vs pulse height gating. The data were analyzed via FlowJo software V.10 (TreeStar, Ashland, Oregon, USA).

Adenovirus production and infection

Adenovirus-control and adenovirus-Adeasy-shTBX21 vectors were constructed by Hanbio Biotechnology (Shanghai, China). The small hairpin RNA sequences for human T-bet are shown in online supplemental table S3. Purified $CD4^+$ T cells were cultured on plates coated with anti-CD3 and anti-CD28 antibodies (2 µg/well, 96-well plate) in the presence of hIL-2 (100 U/mL) for 48 hours. Then, the activated $CD4^+$ T cells were infected with adenovirus in Roswell Park Memorial Institute (RPMI) 1640 medium (100 µL/well) supplemented with polybrene (6 µg/mL) at a multiplicity of infection of 500 at 37°C for 4 hours, and an equal volume of fresh medium was added, resulting in a final volume of 200 µL per well for an additional 8 hours. The transduced cells were then incubated with fresh RPMI 1640 and stimulated with anti-CD3/28 antibodies and hIL-2 for the indicated time intervals.

Culture of patient-derived lung cancer explants

The culture of tumor explants was performed as previously described.[17] In brief, tumors were cut into 2–3 mm^3 cubes or 400 µm-thick slices and randomly added to Dulbecco's Modified Eagle Medium (DMEM) supplemented with 10% heat-inactivated Fetal Bovine Serum (FBS), 100 U/mL penicillin, and 0.1 mg/mL streptomycin. The explants were subsequently cultured in the presence of the indicated stimuli, including 2 µg/mL anti-CD3, 1 µg/mL anti-CD28, 10 µg/mL anti-PD-1, 0.5 µg/mL anti-CD85j, and 10 µg/mL anti-CD4 antibodies with or without the 20 µM phosphatidylinositol 3-kinase (PI3K) inhibitor LY294002. The explants were treated for 24 hours at 37°C. The TILs were subsequently collected for flow cytometric analysis. The sections were fixed with 4% paraformaldehyde for immunohistochemical staining, and the expression of cleaved caspase-3, a cell death marker, was quantified.

Animal model

C57BL/6 mice were purchased from GemPharmatech (Nanjing, China). The mice were housed in specific pathogen-free facilities. All the animal experiments were performed under standard laboratory conditions at the Tongji Hospital Laboratory Animal Center. C57BL/6 mice (6–8 weeks old) were inoculated subcutaneously with 1×10^6 Lv-mCtrl-LLC cells or Lv-mCIITA-LLC cells in the right flank. Immunotherapy was initiated when the tumor volume reached ≈ 50 mm^3. The mice were randomly grouped and treated with isotype control (i.p. 10 mg/kg) or anti-PD-L1 antibody (i.p. 10 mg/kg) on days 8, 11, and 14 (n=8 mice per group). To deplete $CD4^+$ T cells or $CD8^+$ T cells, the mice were treated with an anti-CD4 mAb (i.p. 10 mg/kg) or an anti-CD8 mAb (i.p. 10 mg/kg), respectively, every 3 days starting 1 week before tumor implantation and until the end of the experiments. To block MHC-II expressed on Lv-mCIITA-LLC, an anti-MHC-II mAbs (i.p. 10 mg/kg) was administered. The tumor size was measured with calipers every 2 days. The tumor volume was calculated with the following equation: tumor volume (mm^3)=length×$width^2$×0.5. The mice were euthanized when the tumor volume reached ≈ 2000 mm^3.

Statistical analysis

GraphPad Prism V.8.0 (GraphPad Software) was used for graphing and statistical analysis. The data in the bar graphs are presented as the means±SEMs. Two-tailed paired or unpaired Student's t-tests and one-way or two-way analysis of variance were performed where appropriate to determine the significance of differences between groups. The statistical significance threshold was set at $p<0.05$.

Additional methods

Detailed information on the isolation of lymphocytes, cell lines and T-cell culture, class II major histocompatibility complex transactivator (CIITA) plasmid construction and transfection, RNA isolation and bulk RNA-seq analysis, immunohistochemical staining and quantification, immunofluorescence confocal microscopy and assessment of $CD4^+$ T-cell cytotoxicity is included in the online supplemental M and M.

RESULTS

Dysfunctional state of intratumoral $CD4^+GzmB^+$ T cells in patients with NSCLC

Granzyme B (GzmB)-expressing $CD4^+$ T cells were detected in PBMCs and TILs via flow cytometry (figure 1A and online supplemental figure S1 A). The proportion of $CD4^+GzmB^+$ T cells among total $CD4^+$ T cells was significantly lower in TILs than in PBMCs, whereas the proportion of $CD8^+GzmB^+$ T cells among $CD8^+$ T cells in TILs was comparable to that in PBMCs. Notably, the proportion of $CD4^+GzmB^+$ T cells among the TILs was associated with that among the PBMCs (online supplemental figure S1B). Moreover, the percentage of $CD4^+GzmB^+$ T cells but not that of $CD8^+GzmB^+$ T cells in TILs was lower than that in paired tumor-adjacent tissues (online supplemental figure S1C).

Predominant $CD4^+GzmB^+$ T cells displayed an effector memory phenotype ($CD45RA^-CCR7^-$) (online supplemental figure S1D). As shown in figure 1B, the majority of $CD4^+GzmB^+$ T cells among both PBMCs and TILs expressed CD57 but lost the expression of CD28, which made them phenotypically similar to senescent T cells.[18 19] Detailed analysis of the expression of cytotoxic effectors revealed that a substantial proportion of $CD4^+GzmB^+$ T cells in TILs expressed granzyme A (GzmA) and

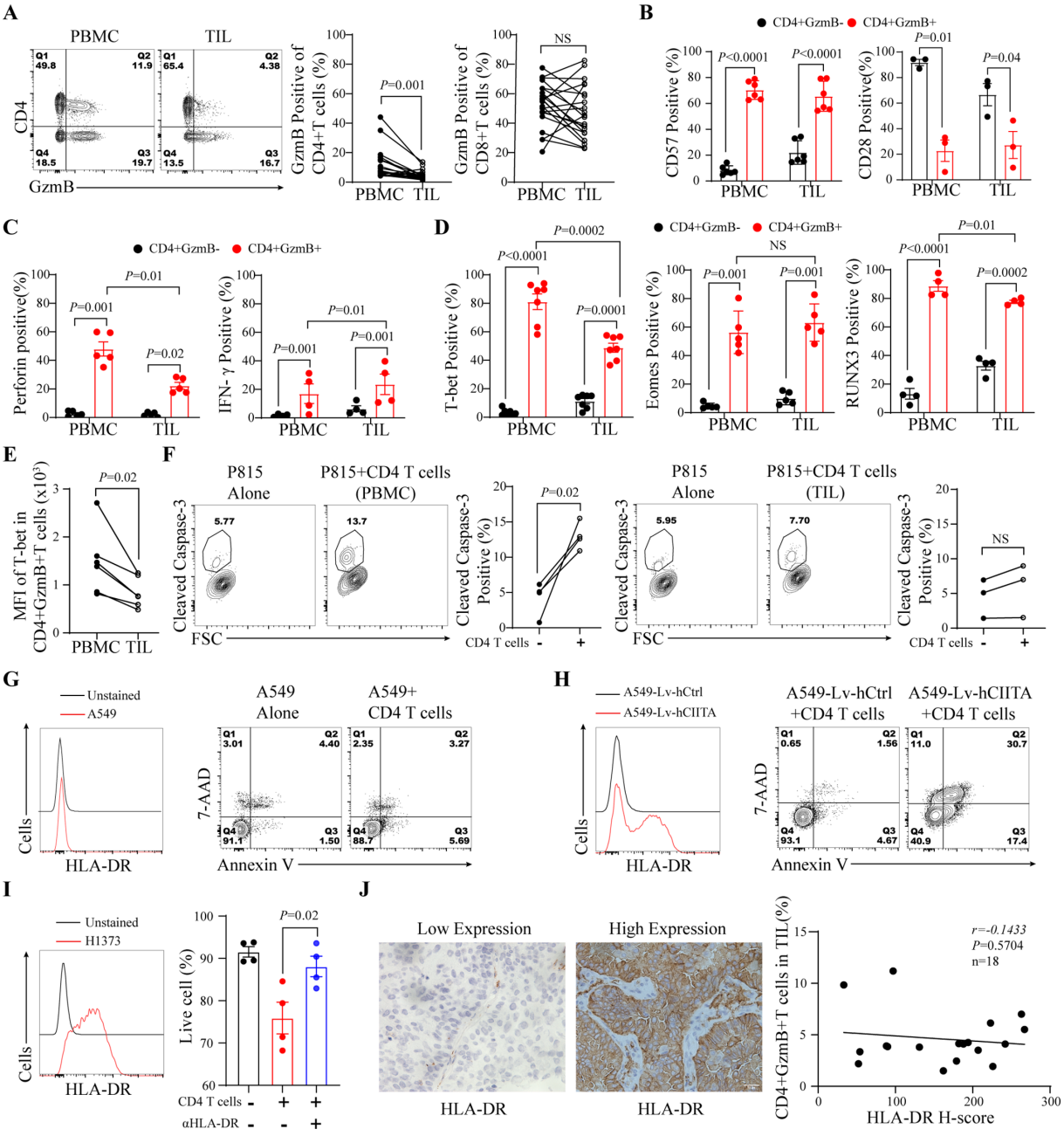

Figure 1 Dysfunctional tumor-infiltrating CD4$^+$GzmB$^+$ T cells in patients with NSCLC. (A) Proportion of GzmB$^+$ cells among CD4$^+$ or CD8$^+$ T cells among the PBMCs and TILs of patients with NSCLC (n=22). (B) Statistical graphs showing the expression of CD57 and CD28 in CD4$^+$GzmB$^-$ T cells and CD4$^+$GzmB$^+$ T cells. (C) Expression of perforin and interferon-γ in CD4$^+$GzmB$^+$ T cells and CD4$^+$GzmB$^-$ T cells from PBMCs and TILs. (D) Expression of T-bet/Eomes/Runx3 in CD4$^+$GzmB$^+$ T cells and CD4$^+$GzmB$^-$ T cells from PBMCs and TILs. (E) Comparison of the MFI of T-bet in CD4$^+$GzmB$^+$ T cells isolated from PBMCs and corresponding tumors (n=6). (F) The cytolytic activity of CD4$^+$ T cells was assessed via a redirected cytotoxicity assay. Statistical graphs showing the proportion of cleaved caspase-3-expressing P815 target cells after co-culture with CD4$^+$ T cells isolated from the PBMCs or tumors of patients with NSCLC. (G, H) The cytolytic activity of CD4$^+$ T cells was assessed in a co-culture of CD4$^+$ T cells with A549 cells (G) or A549 cells transfected with Lv-Ctrl or Lv-CIITA (H) for 24 hours, as described in the Materials and Methods section. Apoptotic cell death was evaluated by staining target cells with annexin V and 7-AAD followed by flow cytometric analysis. (I) A representative histogram showing HLA-DR expression in H1373 cells. The statistical graphs display the percentage of live H1373 target cells after they were co-cultured with CD4$^+$ T cells in the presence or absence of the anti-HLA-DR antibody for 24 hours. (J) Analysis of the correlation between the expression levels of HLA-DR and the proportion of CD4$^+$GzmB$^+$ T cells in tumors. Scale bars=50 µm. The data are shown as the means±SEMs. Statistical significance was determined via paired Student's t-test for A, E and F, two-way analysis of variance (ANOVA) for B–D, and one-way ANOVA for I. Eomes, eomesodermin; GzmB, granzyme B; IFN, interferon; NSCLC, non-small cell lung cancer; PBMC, peripheral blood mononuclear cell; RUNX3, RUNX family transcription factor 3; TILs, tumor-infiltrating lymphocytes; 7-AAD, 7-aminoactinomycin D; HLA-DR, human leukocyte antigen-DR; T-bet, T-box transcription factor 21; MFI, mean fluorescence intensity.

granzyme K (GzmK), whereas some $CD4^+GzmB^+$ T cells in PBMCs expressed GzmA, and a few of them expressed GzmK (online supplemental figure S1E). The majority of $CD4^+GzmB^+$ T cells among PBMCs expressed perforin. A significantly reduced proportion of perforin-expressing $CD4^+GzmB^+$ T cells was observed in TILs. Finally, some $CD4^+GzmB^+$ T cells among both PBMCs and TILs expressed IFN-γ (figure 1C).

Next, we examined the expression of the transcription factors T-bet, Eomes, and Runx3, which are needed for differentiating cytolytic T cells, in $CD4^+GzmB^+$ T cells. As shown in figure 1D, the majority of $CD4^+GzmB^+$ T cells among both PBMCs and TILs expressed Eomes and Runx3, whereas the proportion of T-bet-expressing $CD4^+GzmB^+$ T cells among TILs was significantly lower than that among PBMCs. Moreover, the expression level of T-bet in $CD4^+GzmB^+$ T cells in TILs was also significantly lower than that in PBMCs (figure 1E).

We then evaluated the cytolytic activity of $CD4^+GzmB^+$ T cells by detecting cleaved caspase-3 in target cells via a flow cytometry analyzer. Purified $CD4^+$ T cells from PBMCs and TILs were co-cultured with anti-CD3 mAb-coated P815 target cells. As shown in figure 1F, the proportion of cleaved caspase-3-positive P815 cells was greater among the cells co-cultured with $CD4^+$ T cells isolated from PBMCs than among those co-cultured with $CD4^+$ T cells from TILs. These results indicate that the cytotoxic activity of intratumoral $CD4^+GzmB^+$ T cells is impaired.

Finally, we examined whether $CD4^+$ T-cell-mediated killing of lung cancer cells requires MHC-II expression in target cells. As shown in figure 1G, $CD4^+$ T cells isolated from PBMCs co-cultured with A549 cells, an human leukocyte antigen-DR (HLA-DR)-negative lung cell line, failed to kill A549 cells. We then transfected A549 cells with CIITA, the master transcriptional regulator of MHC-II genes, via a lentiviral vector system and subsequently, co-cultured the resulting A549 cells with $CD4^+$ T cells. An increased level of tumor cell death was observed in the co-culture of $CD4^+$ T cells with MHC-II-overexpressing A549 cells compared with that in the co-culture of $CD4^+$ T cells with control A549 cells (figure 1H). Moreover, when $CD4^+$ T cells were co-cultured with the H1373 cell line, which expresses cell-intrinsic HLA-DR, the number of viable H1373 cells was reduced. This effect was abrogated when the co-cultured cells were treated with an antibody against HLA-DR (online supplemental figure S1F and figure 1I). Similar to human lung cancer cell lines, NSCLC tumor cells heterogeneously express HLA-DR. These results indicate that the cytotoxic $CD4^+$ T-cell-mediated killing of tumor cells is MHC-II restricted. Notably, no correlation between HLA-DR expression in tumor cells and the proportion of intratumoral $CD4^+GzmB^+$ T cells was observed (figure 1J), nor was there a correlation between the number of $CD8^+GzmB^+$ T cells and the level of MHC-I expressed by tumor cells (online supplemental figure S1G).

IL-15 RESTORES INTRATUMORAL $CD4^+GZMB^+$ T-CELL FUNCTIONS BY ENHANCING T-BET EXPRESSION

Several studies have reported that IL-15 increases GzmB and perforin expression in $CD8^+$ T cells.[20 21] Moreover, IL-15 preferentially increases expansion and improves the effector function of intratumoral $CD8^+CD57^+$ T cells rather than that of $CD8^+CD57^-$ T cells.[22] We previously revealed that human lung cancer cells express a significant amount of IL-15, and the responsiveness of tumors to immunotherapy is associated with the level of IL-15 expressed by tumor cells.[23] For these reasons, we examined whether IL-15 is capable of enhancing the cytotoxic effector function of intratumoral $CD4^+GzmB^+$ T cells. As shown in online supplemental figure S2A and figure 2A, the level of IL-15 expressed by tumor cells was strongly correlated with the proportion of intratumoral $CD4^+GzmB^+$ T cells. Moreover, stimulation of PBMCs or TILs with IL-15 led to an increase in the proportion of $CD4^+GzmB^+$ T cells among $CD4^+$ T cells (figure 2B). Detailed analysis revealed that IL-15 preferentially increased the expression of Ki-67 and perforin in $CD4^+GzmB^+$ T cells compared with that in $CD4^+GzmB^-$ T cells (figure 2C,D). Interestingly, we found that $CD4^+GzmB^+$ T cells ex vivo expressed higher levels of IL-15Rα than their counterparts did (online supplemental figure S2B), and stimulation of TILs and PBMCs with anti-CD3/anti-CD28 antibodies further increased the level of IL-15Rα in $CD4^+GzmB^+$ T cells (online supplemental figure S2C). For these reasons, we used a combination of IL-15 and anti-CD3/CD28 mAbs to stimulate TILs and PBMCs. As shown in figure 2E, stimulation of PBMCs and TILs with the combination treatment resulted in a robust increase in the proportion of $CD4^+GzmB^+$ T cells among the total $CD4^+$ T cells.

As the transcription factors T-bet, Eomes, and Runx3 are required for the differentiation and effector function of cytolytic T cells,[24–26] we therefore examined whether and how IL-15 and TCR stimulation affect the expression of these transcription factors. As shown in figure 2F,G, IL-15 alone or in combination with TCR stimulation significantly increased T-bet and Runx3 expression in $CD4^+GzmB^+$ T cells in TILs compared with that in untreated cells. Similar expression patterns were observed in $CD4^+GzmB^+$ T cells from PBMCs (online supplemental figure S2D,E). Interestingly, the addition of IL-15 significantly decreased rather than increased Eomes expression in $CD4^+GzmB^+$ T cells from TILs (figure 2H) and PBMCs (online supplemental figure S2F). Next, we aimed to understand the interaction between T-bet and Runx3 and their roles in the IL-15-mediated restoration of cytotoxic $CD4^+$ T-cell functions. Kinetic analysis revealed that T-bet but not Runx3 expression in $CD4^+$ T cells was increased at 8 hours after stimulation (online supplemental figure S2G). Next, we examined whether T-bet regulates Runx3 expression, as reported by others.[27] As shown in figure 2I T-bet knockdown led to a decrease in Runx3 expression in $CD4^+$ T cells in response to IL-15 and TCR stimulation. More importantly, T-bet knockdown in $CD4^+$ T cells significantly decreased the levels of GzmB and perforin

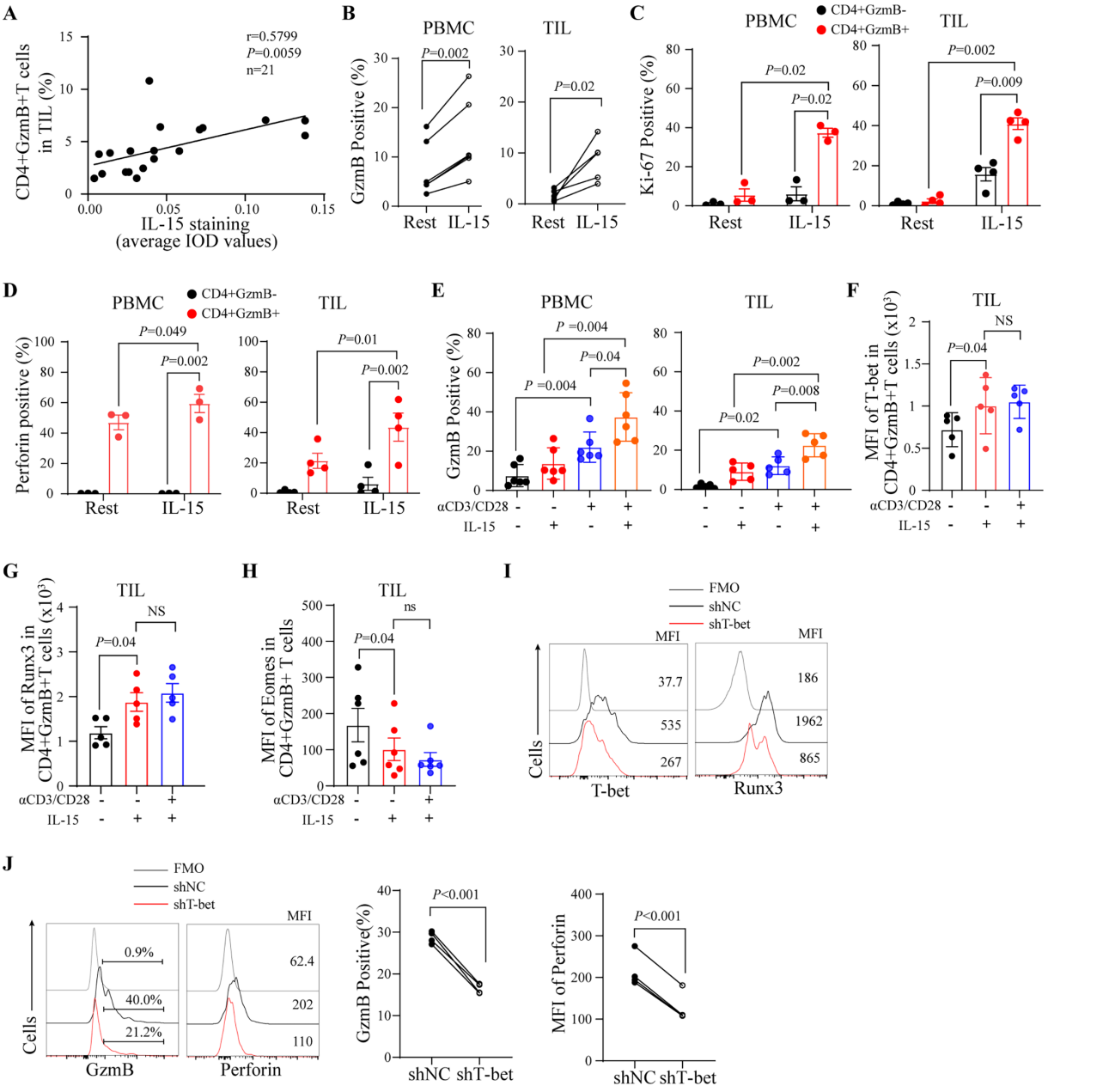

Figure 2 IL-15 restores intratumoral CD4$^+$GzmB$^+$ T-cell functions by enhancing T-bet expression. (A) Correlation analysis of IL-15 expression and the proportion of CD4$^+$GzmB$^+$ T cells in tumors from patients with NSCLC. (B) Percentage of CD4$^+$GzmB$^+$ T cells among CD4$^+$ T cells with or without (Rest) IL-15 (10 ng/mL) stimulation for 3 days. (C, D) The expression of Ki-67 and perforin in CD4$^+$GzmB$^+$ T cells and their counterparts after stimulation of CD4$^+$ T cells with IL-15 or untreated (Rest) for 3 days was analyzed via flow cytometry. (E) The percentage of CD4$^+$GzmB$^+$ T cells among CD4$^+$ T cells was analyzed via flow cytometry after PBMCs or TILs were treated with IL-15 alone or in combination with an anti-CD3 antibody (1 µg/mL) and an anti-CD28 antibody (0.5 µg/mL) for 3 days. (F–H) The MFIs of T-bet, Runx3 and Eomes in CD4$^+$GzmB$^+$ T cells isolated from TILs were analyzed after the simulation of CD4$^+$ T cells with IL-15 alone or in combination with anti-CD3/CD28 for 3 days. (I) Purified CD4$^+$ cells isolated from PBMCs were transfected with shRNA-T-bet or shRNA-NC for 12 hours, as described in the Materials and Methods section, and subsequently treated with IL-15 and anti-CD3/CD28 antibodies for an additional 48 hours. The expression levels of T-bet and Runx3 were assessed by flow cytometry. (J) Histograms showing the expression levels of GzmB and perforin in CD4$^+$ T cells after T-bet was knocked down. The data are shown as the means±SEMs. Statistical significance was determined via paired Student's t-tests for B and J; two-way analysis of variance (ANOVA) for C and D; and one-way ANOVA for E–H. Eomes, eomesodermin; GzmB, granzyme B; IL, interleukin; NSCLC, non-small cell lung cancer; PBMC, peripheral blood mononuclear cell; RUNX3, RUNX family transcription factor 3; TILs, tumor-infiltrating lymphocytes; T-bet, T-box transcription factor 21; MFI, mean fluorescence intensity.

compared with those in CD4+ T cells transduced with Ctrl-shRNA (figure 2J).

The signal transducer and activator of transcription 5 and AKT pathways are involved in the IL-15-mediated restoration of CD4+GzmB+ functions

To determine the underlying mechanism by which IL-15 regulates T-bet expression, we first examined IL-15-mediated signal transduction in CD4+ T cells. As shown in figure 3A, IL-15 activated the signal transducer and activator of transcription 5 (STAT5) pathway in CD4+ T cells, as evidenced by increased STAT5 phosphorylation. Surprisingly, the inhibition of STAT5 activity by STAT5-IN-1 reduced the proportion of CD4+GzmB+ T cells among CD4+ T cells but did not affect T-bet expression

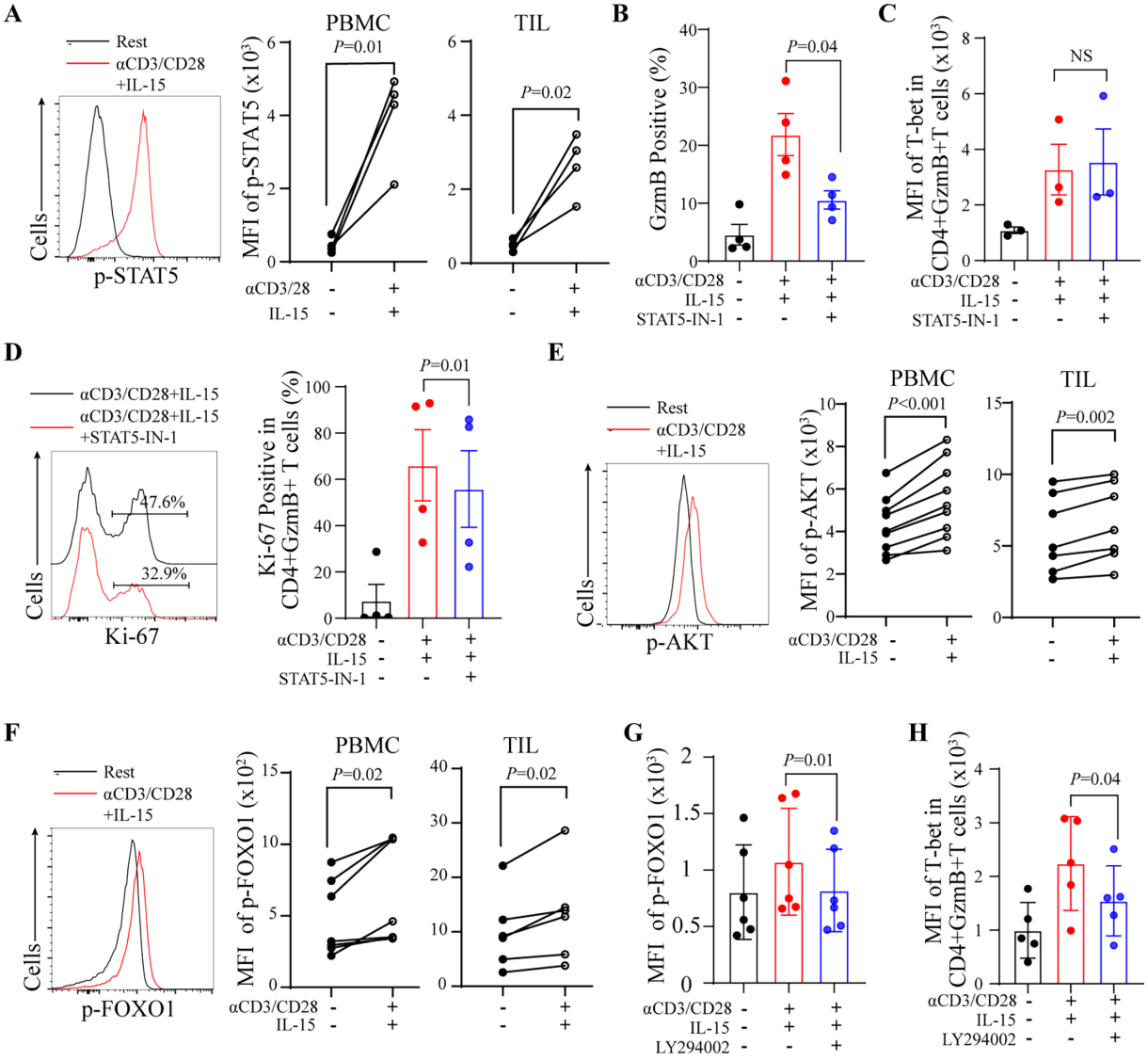

Figure 3 The STAT5 and AKT pathways are involved in the restoration of CD4+GzmB+ functions by IL-15. (A) Phosphorylated STAT5 levels in CD4+ T cells after stimulation with the indicated stimuli for 1 hour were assessed via flow cytometry. (B) CD4+ T cells were treated with or without anti-CD3/CD28 antibodies plus IL-15 in the presence or absence of the STAT5 inhibitor STAT5-IN-1 (50 µM) for 24 hours. The percentage of CD4+GzmB+ T cells was analyzed via flow cytometry. (C, D) Statistical graphs showing the MFI of T-bet and the percentage of Ki67-positive CD4+ GzmB+ T cells after treatment with the indicated stimuli in the presence or absence of STAT5-IN-1. (E, F) Representative histogram and statistical graphs showing the levels of phosphorylated AKT and FOXO1 in CD4+ T cells after treatment with IL-15 and anti-CD3/CD28 antibodies for 1 hour. (G) CD4+ T cells were treated as described in (F) with or without the PI3K inhibitor LY294002 (10 µM) for 1 hour. The level of phosphorylated Foxo1 was assessed via flow cytometry (n=5). (H) The MFI of T-bet in CD4+GzmB+ T cells was analyzed by flow cytometry after stimulation of CD4+ T cells with IL-15 alone or in combination with anti-CD3/CD28 in the presence or absence of the PI3K inhibitor LY294002 (10 µM) for 24 hours. The data are shown as the means±SEMs. Statistical significance was determined via paired Student's t-tests for A, E and F and one-way analysis of variance for B, C, D, G and H. FOXO1, forkhead box O1; GzmB, granzyme B; IL, interleukin; PBMC, peripheral blood mononuclear cell; PI3K, phosphatidylinositol 3-kinase; STAT5, signal transducer and activator of transcription 5; TILs, tumor-infiltrating lymphocytes; AKT, Protein Kinase B; MFI, mean fluorescence intensity.

in CD4+GzmB+ T cells after stimulation with IL-15 and anti-CD3/CD28 mAbs (figure 3B,C); moreover, under the same conditions, STAT5-IN-1 significantly suppressed Ki-67 expression in CD4+GzmB+ T cells (figure 3D). These data indicate that the IL-15-mediated activation of STAT5 is involved in increasing the proliferative capability but not the cytotoxic potential of CD4+GzmB+ T cells.

In addition to activating the STAT5 pathway, stimulation with IL-15 alone or in combination with anti-CD3/CD28 mAbs induced Protein Kinase B (AKT) activation (online supplemental figure S3A and figure 3E). Several studies have reported that the activation of AKT inhibits the activity of the transcription factor forkhead box O1 (FOXO1) by phosphorylating FOXO1 and leading to its nuclear exclusion, thereby abrogating its transcriptional repression of T-bet expression.[28–30] As expected, the levels of phosphorylated FOXO1 were increased in CD4+ T cells on stimulation with anti-CD3/CD28 mAbs and IL-15 (figure 3F). As shown in online supplemental figure S3B, FOXO1 nuclear exclusion occurred in CD4+ T cells after stimulation with anti-CD3/CD28 mAbs and IL-15. The addition of the PI3K inhibitor LY294002 abrogated FOXO1 phosphorylation induced by stimulation of CD4+ T cells with anti-CD3/CD28 mAbs and IL-15 (figure 3G), and consequently, as shown in figure 3H T-bet expression was significantly reduced in CD4+ T cells. These results indicate that activation of the PI3K-AKT pathway by IL-15 alone or by IL-15 in combination with TCR stimulation increases T-bet expression by inhibiting the nuclear translocation of FOXO1 in CD4+ T cells. The addition of LY294002 also abrogated the increase in Ki-67 expression induced by stimulation of CD4+ T cells with anti-CD3/CD28 mAbs and IL-15 (online supplemental figure S3C), indicating that the AKT pathway is involved in improving the proliferative capability of these cells.

SLC7A5 upregulation is essential for the effector function of CD4+GzmB+ T cells

To further explore the effect of IL-15 on CD4+GzmB+ T cells, unbiased RNA-seq was performed on CD4+ T cells that were purified from PBMCs and either stimulated with IL-15 plus anti-CD3/CD28 mAbs or not stimulated. As shown in online supplemental figure S4A, the unsupervised Principal components analysis (PCA) score plot clearly revealed that IL-15-treated and untreated CD4+ T cells formed separate clusters. All differentially expressed genes (DEGs) are visualized via a volcano plot (online supplemental figure S4B), and 8,495 DEGs (q value<0.05) were identified, of which 3,279 were upregulated and 5,216 were downregulated. The heatmap in online supplemental figure S4C displays the top 100 differentially expressed genes between the two groups and the information of these genes is listed in online supplemental table S4. Bioinformatics analysis of the DEGs revealed that they were associated with amino acid biosynthesis and metabolism (online supplemental figure S4D,E). T-cell activation and differentiation are coupled with rapid amino acid uptake, which is dependent on amino acid transporters.[31 32] Therefore, we examined whether stimulation of CD4+ T cells with IL-15 plus anti-CD3/CD28 mAbs affects amino acid transporter expression. As shown in online supplemental figure S4F, a heatmap revealed that the expression of amino acid transporters, including SLC1A5 (ASCT2), SLC7A1, and particularly SLC7A5 (LAT1), was greater in CD4+ T cells stimulated with IL-15 and anti-CD3/CD28 mAbs than in unstimulated CD4+ T cells.

We then evaluated the expression of SLC7A5 at the protein level in CD4+ T cells on stimulation. Flow cytometry analysis revealed that, compared with that in unstimulated CD4+ T cells, the expression level of SLC7A5 in CD4+ T cells was significantly increased on stimulation with IL-15, and SLC7A5 expression was further increased when CD4+ T cells were stimulated with the combination of IL-15 and anti-CD3/CD28 mAbs (online supplemental figure S5A). Next, we investigated whether SCL7A5 is differentially expressed between CD4+GzmB+ T cells and CD4+GzmB− T cells. As shown in figure 4A, when CD4+ T cells were stimulated with IL-15 and anti-CD3/CD28 mAbs, CD4+GzmB+ T cells expressed higher levels of SLC7A5 than their counterparts did. Notably, the level of SLC7A5 expression was greater in CD4+GzmB+ T cells ex vivo than in CD4+GzmB+ T cells. Moreover, CD4+GzmB+ T cells in PBMCs expressed high level of SLC7A5 compared with those in TILs (figure 4B), and a similar expression pattern of SLC7A5 was also observed in CD8+GzmB+ T cells (figure 4C). These results led us to speculate that SLC7A5 upregulation might be associated with the cytolytic function of CD4+ T cells. As shown in figure 4D, the use of JPH203, an inhibitor of SLC7A5, even at a low dose, which had little effect on IFN-γ expression, significantly reduced the expression of T-bet and Runx3 in CD4+ T cells on stimulation with IL-15 and TCR/CD28; moreover, GzmB expression was also decreased in CD4+ T cells (figure 4E). These data indicate that cytotoxic CD4+ T cells are sensitive to SLC7A5 inhibition.

Next, we determined whether SLC7A5 affects IL-15-mediated signaling in CD4+T cells. As shown in online supplemental figure S5B–D, the addition of the SLC7A5 inhibitor JPH203 did not affect the IL-15-mediated activation of STAT5 or the AKT-FOXO1 axis. Upregulation of SLC7A5 increases the uptake of neutral amino acids, which activate mammalian target of rapamycin complex 1 (mTORC1) and its downstream p-S6.[33] As shown in figure 4F, inhibition of SLC7A5 led to a decrease in ribosomal protein S6 phosphorylation in CD4+T cells after IL-15 stimulation. mTORC1 activation has been shown to regulate T-bet expression.[34] The addition of the mTORC1 inhibitor rapamycin led to the downregulation of both T-bet and GzmB expression in cells after stimulation with IL-15 and anti-CD3/CD28 mAbs (figure 4G,H). Notably, mTORC1 inhibition did not affect the levels of p-AKT or p-FOXO1 in cells in response to IL-15 stimulation (online supplemental figure S5E and 5F). These findings indicate that the induction of SLC7A5 by IL-15 increases

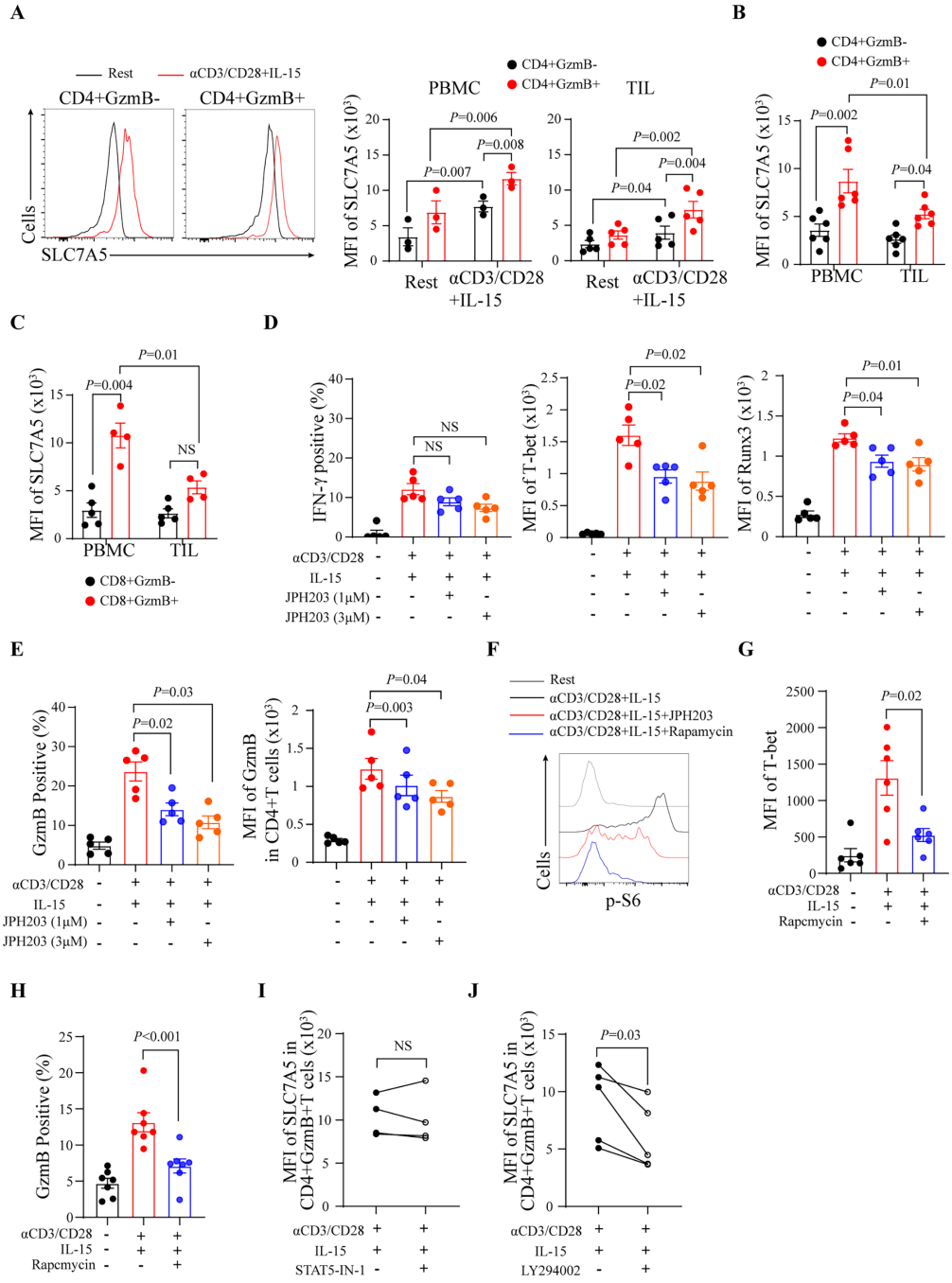

Figure 4 IL-15-induced SLC7A5 expression in CD4⁺ T cells is essential for increasing the proportion of CD4⁺GzmB⁺ T cells. (A) Representative histogram and statistical graphs of SLC7A5 expression in CD4⁺GzmB⁻ and CD4⁺GzmB⁺ T cells after the cells were stimulated with IL-15 and anti-CD3/CD28 antibodies plus IL-15 for 24 hours. (B, C) SLC7A5 expression in CD4⁺ T cells (B) and CD8⁺ T cells (C) ex vivo was analyzed by flow cytometry. (D) Statistical graphs showing the expression levels of IFN-γ, T-bet and Runx3 in CD4⁺ T cells treated with IL-15 and anti-CD3/CD28 mAbs in the presence of the indicated concentrations of the SLC7A5 inhibitor JPH203 for 72 hours. (E) Statistical graphs showing the percentage of GzmB⁺ and MFI of GzmB among CD4⁺ T cells treated with IL-15 and anti-CD3/CD28 mAbs in the presence of the indicated concentrations of the SLC7A5 inhibitor JPH203 for 72 hours. (F) MFI of p-S6 was analyzed after stimulation of CD4⁺ T cells with IL-15 and anti-CD3/CD28 antibodies in the presence or absence of JHPH203 or rapamycin for 24 hours. (G, H) T-bet (G) and GzmB (H) levels after stimulation of CD4⁺ T cells with IL-15 in combination with anti-CD3/CD28 antibodies in the presence or absence of rapamycin for 24 hours. (I, J) PBMCs or TILs were treated separately with the inhibitors LY294002 (10 μM) and STAT5-IN-1 (50 μM) with anti-CD3/CD28 mAbs plus IL-15 for 24 hours. SLC7A5 expression was subsequently assessed in CD4⁺GzmB⁺ T cells via flow cytometry. The data are shown as the means±SEMs. Statistical significance was determined via paired Student's t-tests for I and J; two-way analysis of variance (ANOVA) for A–C; and one-way ANOVA for D, E, G and H. GzmB, granzyme B; IFN, interferon; IL, interleukin; PBMC, peripheral blood mononuclear cell; RUNX3, RUNX family transcription factor 3; SLC7A5, solute carrier family 7 member 5; STAT5, signal transducer and activator of transcription 5; TILs, tumor-infiltrating lymphocytes; T-bet, T-box transcription factor 21; MFI, mean fluorescence intensity; mAb, monoclonal antibody.

CD4+CTL activity via the activation of mTORC1 but not the AKT-FOXO1 axis.

Finally, we sought to determine the underlying mechanism of SLC7A5 upregulation. As shown in figure 4I, the addition of the STAT5 inhibitor STAT5-IN-1 did not affect SLC7A5 expression in CD4+GzmB+ T cells induced by the combination of IL-15 and anti-CD3/CD28 mAb stimulation; however, given the same stimuli in the presence of the PI3K inhibitor LY294002, SLC7A5 upregulation in CD4+GzmB+ T cells was abrogated (figure 4J). Notably, on stimulation of CD4+ T cells with TCR/CD28 and IL-15, the level of phosphorylated AKT was significantly increased in CD4+GzmB+ T cells but not in CD4+GzmB− T cells in tumors (online supplemental figure S5G). These results indicate that activation of the PI3K-AKT pathway in CD4+GzmB+ T cells by stimulation with TCR/CD28 and IL-15 is responsible for SLC7A5 upregulation, which in turn further contributes to the restoration of the effector function of these cells.

Dual blockade of PD-1 and CD85j restores CD4+GzmB+ T-cell cytotoxic activities against tumor cells in a model of patient-derived NSCLC explants

T-cell activation is negatively regulated by interactions between immune checkpoints (ICs) expressed on T cells and the ligands for ICs expressed on tumor cells.[35–38] Among ICs, PD-1 is the most recognized molecule expressed in tumor-infiltrating T cells. As CD4+GzmB+ T cells in tumors are dysfunctional, we examined PD-1 expression in these cells. As shown in figure 5A, intratumoral CD4+ T cells expressed PD-1, and the expression level of PD-1 in CD4+GzmB+ T cells was greater than that in CD4+GzmB− T cells. Moreover, PD-1 expression was even higher in CD4+GzmB+ T cells than in CD8+GzmB+ T cells (online supplemental figure S6A).

Patient-derived explant (PDE) models have been used in preclinical tumor research to investigate treatment strategies, including immunotherapy.[39] We then used a PDE model to assess whether PD-1 blockade affects intratumoral CD4+GzmB+ T cells. To establish the PDE model, we first evaluated the viability of PDEs ex vivo or in vitro cultured in DMEM with 10% FBS for 24 hours to 48 hours via immunohistochemical staining with antibodies against cleaved caspase-3, a marker of apoptotic cell death. As shown in online supplemental figure S6B, cleaved caspase-3-immunoreactive tumor cells were rarely observed in PDEs ex vivo or cultured in vitro without treatment. Once the PDE model was established, we cultured PDEs with anti-CD3/CD28 antibodies alone or in combination with anti-PD-1 antibodies for 24 hours. Flow cytometry analysis of T cells isolated from explants revealed that the proportion of CD4+GzmB+ T cells among total CD4+ T cells was significantly greater in PDEs treated with the combination of anti-CD3/CD28 and anti-PD-1 antibodies than in PDEs treated with anti-CD3/CD28 antibodies alone (figure 5B). Moreover, the number of cleaved caspase-3-positive tumor cells was significantly associated with the proportion of CD4+GzmB+ T cells when PDEs were treated with a combination of anti-CD3/CD28 and anti-PD-1 antibodies (figure 5C). Furthermore, blocking CD4+ T-cell activation with an anti-CD4 mAb (RPAA-T4) significantly compromised the antitumor effects of the combination treatment, as evidenced by a decrease in the number of apoptotic tumor cells (figure 5D and online supplemental figure S6C), indicating the importance of CD4+ T-cell-mediated antitumor immunity in PD-1 blockade.

As shown in figure 2A–C, the IL-15 expression level in tumor cells was associated with the number of intratumoral CD4+GzmB+ T cells, and we wondered whether the IL-15 expression level in PDEs affects the antitumor effects of PD-1 blockade. As shown in figure 5E, the number of cleaved caspase-3-positive tumor cells was strongly associated with the level of IL-15 in tumors. Moreover, a total of 14 PDEs were divided into two groups according to the median expression level of IL-15 in tumor cells (IL-15high, n=7; IL-15low, n=7) (figure 5F), and the percentage of CD4+GzmB+ T cells in IL-15high PDEs but not in IL-15low PDEs increased after combination treatment (figure 5G). In addition to IL-15 levels, the number of cleaved caspase-3-positive tumor cells in PDEs after combination treatment with anti-CD3/CD28 and anti-PD-1 antibodies was strongly associated with MHC-I and MHC-II expression levels in tumors (online supplemental figure S6D,E), which was consistent with the clinical findings of other studies.[40]

In addition to PD-1, other ICs were also examined in CD4+GzmB+ T cells. CD85j was almost exclusively expressed in CD4+GzmB+ T cells but not in CD4+GzmB− T cells, whereas the expression patterns of T-cell immunoreceptor with Ig and ITIM domains (TIGIT) and lymphocyte activating gene-3 in CD4+GzmB+ T cells were similar to those in their counterparts (figure 5H). We then evaluated the antitumor effects of CD85j blockade and its effect on CD4+GzmB+ T cells. As shown in figure 5I, blocking CD85j significantly increased the number of CD4+GzmB+ T cells; however, the number of CD8+GzmB+ T cells in PDEs was not affected by CD85j blockade (online supplemental figure S6F). Moreover, CD85j was preferentially expressed in CD4+GzmB+ T cells but not in CD8+GzmB+ T cells (online supplemental figure S6G). Given that TIGIT is undoubtedly a potential target for immunotherapy,[41] and is highly expressed by CD4+ TILs, although its expression levels are not related to GzmB expression, we examined whether a TIGIT blocker promotes CD4+GzmB+ T cell expansion. TIGIT blockade did not increase the proportion of CD4+GzmB+ T cells among CD4+ TILs (online supplemental figure S6H). Interestingly, as shown in figure 5J, PD-1 and CD85j demonstrated almost mutually exclusive expression in CD4+GzmB+ T cells. Additionally, the CD85j ligand HLA-G was heterogeneously expressed by lung tumor cells (online supplemental figure S6I). We therefore speculated that dual blockade of PD-1 and CD85j might restore the function of CD4+GzmB+ T cells and increase the antitumor effect.

To test our hypothesis, we evaluated the status of CD4+GzmB+ T cells in explants after treatment with

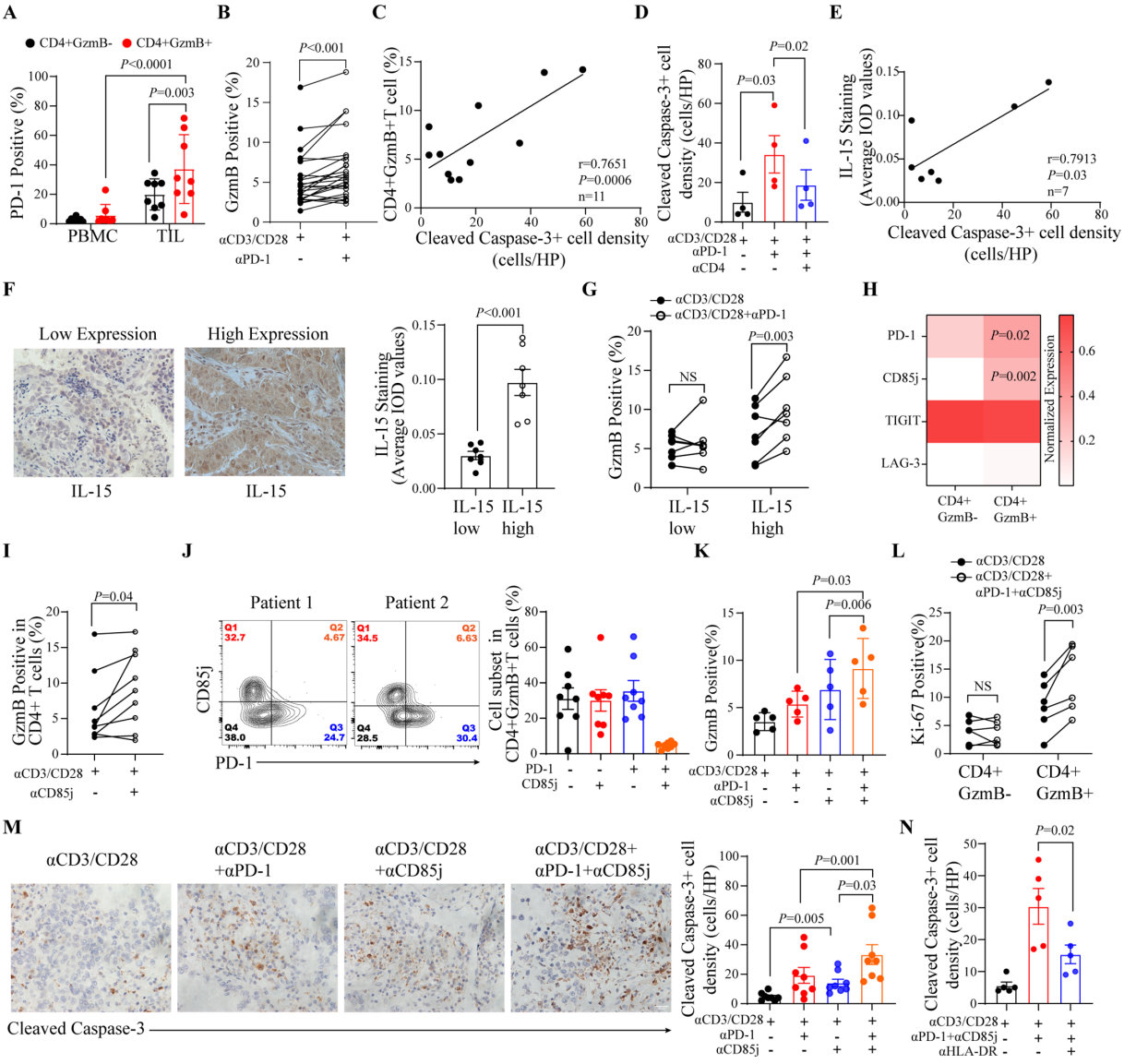

Figure 5 Dual blockade of PD-1 and CD85j synergistically promotes the antitumor immunity of intratumoral CD4$^+$GzmB$^+$ T cells. (A) PD-1 expression in CD4$^+$GzmB$^-$ and CD4$^+$GzmB$^+$ T cells from PBMCs and TILs was analyzed by flow cytometry (n=8). (B) Statistical graphs of GzmB expression in CD4$^+$ T cells after explants were stimulated with anti-CD3/CD28 mAbs in the presence or absence of a PD-1 neutralizing antibody for 24 hours (n=25). (C) Analysis of the correlation between the proportion of CD4$^+$GzmB$^+$ T cells and the number of cleaved caspase-3-positive tumor cells in the explants that were treated as described in (B). (D) Statistical graphs of cleaved caspase-3-positive cells in explants after treatment with anti-CD3/CD28 and anti-PD-1 mAbs in the presence or absence of a CD4 neutralizing antibody (n=4). (E) Correlation analyses between the expression of IL-15 and the number of cleaved caspase-3-positive cells in explants after treatment with anti-CD3/CD28 and anti-PD-1 mAbs. (F) The tumor explants were categorized into two groups on the basis of the median level of expression of IL-15 in tumors as assessed by immunohistochemistry (IHC). (G) The percentage of CD4$^+$GzmB$^+$ T cells among CD4$^+$ T cells in IL-15^{high} versus IL-15^{low} explants that were treated as described in (B) (n=7). (H) Heatmap showing the normalized expression of exhaustion markers in CD4$^+$GzmB$^-$ and CD4$^+$GzmB$^+$ T cells from TILs. (I) Explants were treated with anti-CD3/CD28 mAbs in the presence or absence of a CD85j neutralizing antibody for 24 hours. The proportion of GzmB$^+$ T cells among CD4$^+$ T cells was analyzed by flow cytometry (n=9). (J) Ex vivo expression patterns of PD-1 and CD85j in CD4$^+$GzmB$^+$ T cells from TILs (n=8). (K, L) Explants were treated with anti-CD3/CD28 antibodies plus anti-PD-1 and anti-CD85j antibodies for 24 hours. The proportions of CD4$^+$GzmB$^+$ T cells among CD4$^+$ T cells (K) and the proportions of Ki-67-expressing (L) CD4$^+$GzmB$^-$ and CD4$^+$GzmB$^+$ T cells were analyzed via flow cytometry. (M) Explants were treated as described in I–K. Cleaved caspase-3-positive tumor cells were analyzed via IHC (n=8). Scale bars=50 µm. (N) Explants were treated as described in I–K. An anti-HLA-DR neutralizing antibody was added to the culture for 24 hours. Cleaved caspase-3-positive tumor cells were analyzed via IHC. The data are shown as the means±SEMs. Statistical significance was determined via Student's t-test for F; paired Student's t-test for B, H and I; two-way analysis of variance (ANOVA) for A, G and L; and one-way ANOVA for D, K, M and N. GzmB, granzyme B; IL, interleukin; LAG3, lymphocyte activating gene-3; PBMC, peripheral blood mononuclear cell; PD-1, programmed cell death protein-1; TIGIT, T-cell immunoreceptor with Ig and ITIM domains; TILs, tumor-infiltrating lymphocytes; MFI, mean fluorescence intensity; HP, higher power; HLA-DR, human leukocyte antigen-DR.

anti-CD3/CD28 antibodies in the presence of anti-PD-1 or anti-CD85j antibodies alone or in combination. The greatest increase in the proportion of $CD4^+GzmB^+$ T cells occurred after the explants were treated with the combination of anti-PD-1 and anti-CD85j antibodies (figure 5K). Moreover, blocking PD-1 and CD85j preferentially increased Ki-67 and T-bet expression in $CD4^+GzmB^+$ T cells but not in $CD4^+GzmB^-$ T cells (figure 5L and online supplemental figure S6J). As shown in figure 5M, dual blockade of PD-1 and CD85j resulted in more cleaved caspase-3 positive tumor cells in PDEs than blockade of PD-1 or CD85j alone. Importantly, the antitumor effect of dual PD-1 and CD85j blockade was abrogated when the PDEs were cultured in the presence of an antibody against HLA-DR (figure 5N). These data demonstrated that dual blockade of PD-1 and CD85j significantly restored intratumoral $CD4^+GzmB^+$ T-cell function by increasing the proliferative capability and cytotoxic potential of T cells in an MHC class II-dependent manner.

Several studies have reported that both PD-1-mediated and CD85j-mediated signaling pathways inhibit PI3K-AKT activation,[42 43] which plays an essential role in regulating the effector function of $CD4^+GzmB^+$ T cells. As shown in online supplemental figure S6K, compared with anti-CD/CD28 antibodies alone, dual PD-1 and CD85j blockade significantly increased the level of phosphorylated AKT in $CD4^+GzmB^+$ T cells but not in $CD4^+GzmB^-$ T cells in PDEs. Moreover, the increase in the number of $CD4^+GzmB^+$ T cells in PDEs cultured with antibodies blocking PD-1 and CD85j was abrogated when the PDEs were cultured with the PI3K inhibitor LY294002 (online supplemental figure S6L), indicating the importance of the AKT pathway in the restoration of $CD4^+GzmB^+$ T-cell function via dual blockade of PD-1 and CD85j.

Cancer cell expression of MHC-II is required for $CD4^+GzmB^+$ T-cell-mediated antitumor immunity in response to PD-L1 blockade therapy

To verify the PDE experimental findings, and specifically to determine the association between MHC-II expressed in tumors and the contribution of antitumor immunity induced by $CD4^+GzmB^+$ T cells in response to PD-1 blockade therapy, we used Lewis lung carcinoma (LLC) cells to establish a subcutaneous tumor mouse model. As shown in online supplemental figure S7A, MHC-II was not expressed in LLC cells. We constructed a CIITA-overexpressing LLC cell line (Lv-mCIITA), which expressed higher levels of MHC-II than control cells did (online supplemental figure S7B). C57BL/6 mice were subsequently injected with Lv-Ctrl-LLC cells or Lv-mCIITA-LLC cells to establish a subcutaneous tumor model, and how these tumors respond to PD-1 blockade therapy was examined.

As shown in figure 6A,B, mice bearing Lv-Ctrl-LLC tumors or Lv-mCIITA-LLC tumors were randomly divided into two groups and administered control isotype IgG or an anti-PD-L1 mAb. In mice bearing Lv-Ctrl-LLC tumors, anti-PD-L1 therapy significantly inhibited tumor growth compared with that in control IgG-treated mice; however, overall survival did not improve with anti-PD-L1 therapy. Interestingly, in mice bearing Lv-mCIITA-LLC tumors, anti-PD-L1 therapy significantly inhibited the growth of MHC-II-expressing LLC tumors and prolonged the survival of tumor-bearing mice compared with those of mice treated with control IgG. Furthermore, as shown in online supplemental figure S7C, the efficacy of anti-PD-L1 therapy was significantly compromised after blocking MHC-II in $CIITA^+$ tumors. These results further confirmed that the better response of $CIITA^+$ tumors to anti-PD-L1 therapy was MHC-II-dependent. Notably, tumor growth was comparable between Lv-Ctrl-LLC tumors and Lv-mCIITA-LLC tumors without anti-PD-1 therapy. These results indicate that MHC-II expression in tumor cells has predictive value for the response to anti-PD-L1 therapy.

To elucidate the underlying mechanism, we first examined the status of tumor-infiltrating T cells in MHC-II-expressing tumors versus those in tumors lacking MHC-II in response to anti-PD-L1 therapy. As shown in online supplemental figure S7D,E, immunohistochemical staining analysis revealed that in tumors lacking MHC-II, anti-PD-L1 therapy increased the number of tumor-infiltrating $CD8^+$ T cells but not the number of tumor-infiltrating $CD4^+$ T cells. Interestingly, in MHC-II-expressing tumors, anti-PD-L1 therapy increased the number of intratumoral $CD8^+$ T cells and $CD4^+$ T cells. Moreover, flow cytometric analysis revealed that in MHC-II-expressing tumors, anti-PD-L1 treatment significantly increased the proportion of $CD4^+$ T cells that expressed T-bet, Runx3, and Eomes; however, anti-PD-L1 treatment did not affect the expression of these transcription factors in $CD4^+$ T cells in tumors lacking MHC-II (figure 6C). Consistent with the data shown in figure 6C, anti-PD-L1 treatment significantly increased the proportion of $CD4^+GzmB^+$ T cells in MHC-II-expressing tumors but not in tumors lacking MHC-II (figure 6D). Additionally, Ki-67 and perforin expression in $CD4^+GzmB^+$ T cells was significantly greater in MHC-II-expressing LLC tumors than in tumors lacking MHC-II after anti-PD-L1 therapy (figure 6E).

Next, we assessed the cytotoxic activity of intratumoral $CD4^+$ T cells after anti-PD-L1 treatment. $CD4^+$ T cells isolated from MHC-II-expressing LLC tumors were co-cultured with Lv-Ctrl-LLC or Lv-mCIITA-LLC cells. As shown in figure 6F, some of the Lv-mCIITA-LLC cells co-cultured with $CD4^+$ T cells underwent apoptosis, whereas the $CD4^+$ T cells failed to kill the Lv-Ctrl-LLC cells.

Unlike the effects on $CD4^+GzmB^+$ T cells (figure 6D), anti-PD-L1 therapy increased the proportion of $CD8^+GzmB^+$ T cells among total intratumoral $CD8^+$ T cells regardless of whether the tumor cells expressed MHC-II molecules (online supplemental figure S7F); moreover, despite an increase in Ki-67 expression, perforin expression was not significantly altered in the $CD8^+GzmB^+$ T cells of MHC-II-expressing tumors after anti-PD-L1 therapy (online supplemental figure S7G). As shown in

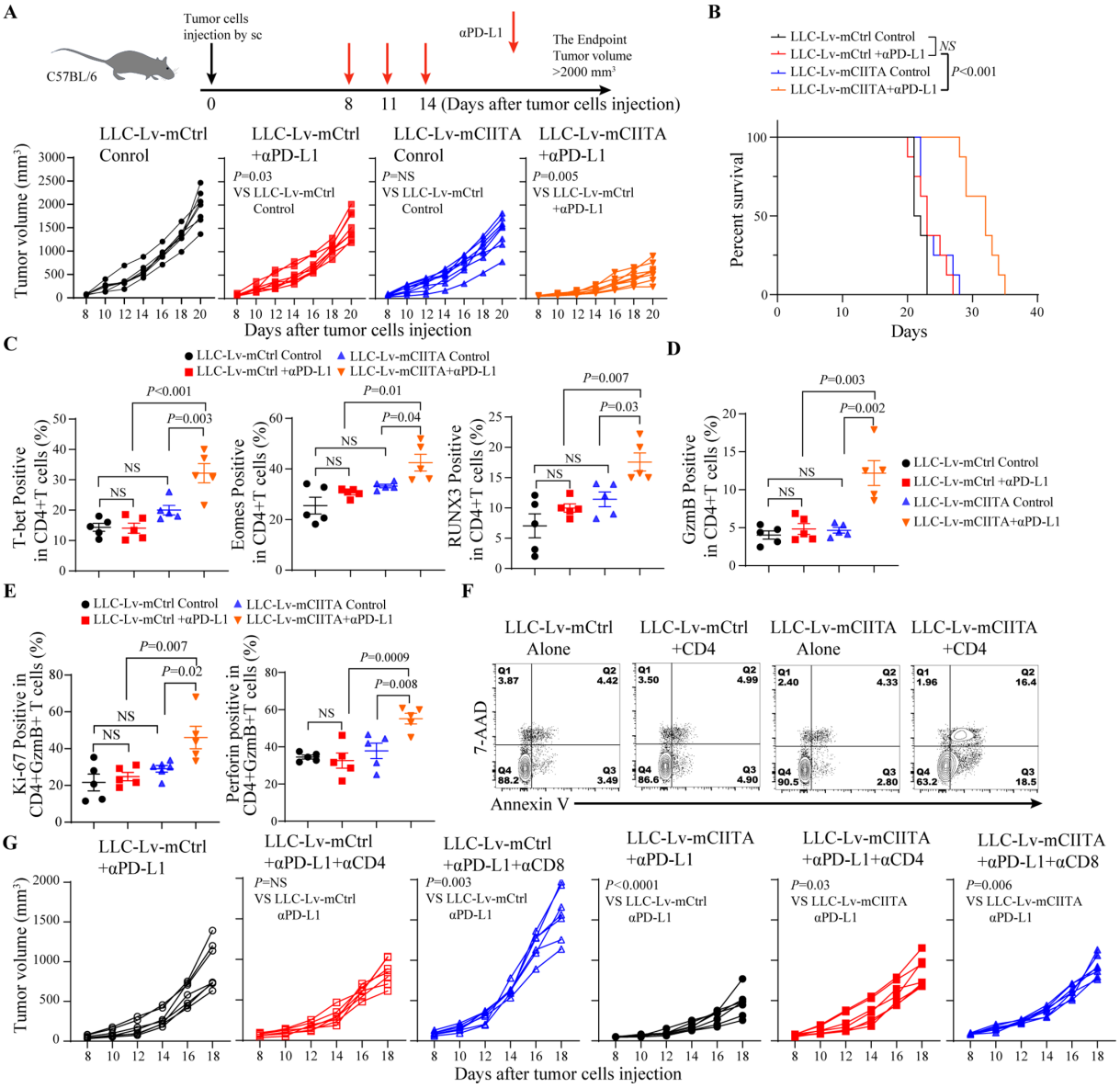

Figure 6 CD4$^+$GzmB$^+$ T-cell-mediated antitumor immunity requires cancer cell-intrinsic expression of major histocompatibility complex II in response to PD-L1 blockade therapy LLC cells transfected with Lv-CIITA or Lv-Ctrl were injected intravenously into C57BL/6 mice. The mice were treated with an isotype control or an anti-PD-L1 antibody (n=8 mice/group). (A) Tumor growth curve data are presented as the mean±SEM. (B) Kaplan-Meier survival curves for mice inoculated with LLC cells that were transfected with Lv-Ctrl-LLC cells or Lv-CIITA and subsequently treated with or without an anti-PD-L1 antibody were generated via the log-rank test. (C, D) The expression levels of transcription factors, including T-bet, Eomes, Runx3 (C) and GzmB (D), in CD4$^+$ T cells were analyzed by flow cytometry (n=5). (E) Statistical graphs showing the proportions of Ki-67-positive or perforin-positive CD4$^+$GzmB$^+$ T cells after the indicated treatments. (F) Cytotoxic activity of intratumoral CD4$^+$ T cells isolated from anti-PD-L1 treated mice was assessed via co-culture of these cells with the indicated LLC cells for 24 hours. Apoptotic death of target LLC cells was assessed via annexin V/7-AAD staining followed by flow cytometric analysis. (G) LLC cells were transfected with Lv-CIITA or Lv-Ctrl and then were injected intravenously into C57BL/6 mice. The mice were treated with an anti-PD-L1 antibody in combination with either an anti-CD4 mAb or anti-CD8 mAb (n=7 mice/group). The tumor growth curve data are presented as the mean±SEM. The data are shown as the means±SEMs. Statistical significance was determined via two-way analysis of variance (ANOVA) for A and G, the log-rank test for B, and one-way ANOVA for C–E. Eomes, eomesodermin; GzmB, granzyme B; LLC, Lewis lung carcinoma; PD-L1, programmed death-ligand 1; RUNX3, RUNX family transcription factor 3; sc, subcutis; mAb, monoclonal antibody; T-bet,T-box transcription factor 21; 7-AAD, 7-aminoactinomycin D.

figure 6G, when CD8$^+$ T cells but not CD4$^+$ T cells were depleted in Lv-Ctrl-LLC tumor-bearing mice, the efficacy of anti-PD-L1 therapy was significantly compromised. These data suggest that CD8$^+$ T cells, but not CD4$^+$ T cells play a crucial role in determining the responsiveness of MHC-II-deficient tumors to anti-PD-L1 therapy. Interestingly, depletion of either CD8$^+$ T cells or CD4$^+$ T cells in Lv-CIITA-LLC tumor-bearing mice resulted in significantly reduced efficacy of anti-PD-L1 therapy, suggesting that the improved efficacy of anti-PD-L1 therapy in

MHC-II-expressing tumors involves both $CD4^+$ T cells and $CD8^+$ T cells.

DISCUSSION

In this study, the state of $CD4^+GzmB^+$ T cells in patients with NSCLC was investigated. We showed that $CD4^+GzmB^+$ T cells among PBMCs but not TILs killed targeted tumor cells in an MHC-II-dependent manner. We then revealed that IL-15 enhanced the proliferative capability and cytotoxic potential of tumor-infiltrated $CD4^+GzmB^+$ T cells. Additionally, dual blockade of PD-1 and CD85j increased the number of intratumoral $CD4^+GzmB^+$ T cells and the effector function of these cells, as demonstrated in the PDE model. Moreover, the $CD4^+GzmB^+$ T-cell-mediated antitumor immune response increased immunotherapy efficacy. This effect relies on tumor cell-intrinsic expression of MHC-II.

We previously showed that IL-15 preferentially increases the cytotoxic activity of terminally differentiated $CD8^+CD57^+$ T cells in patients with NSCLC.[22] IL-15 has also been shown to enhance the expansion and effector functions of cytotoxic $CD4^+CD28^-$ T cells in chronic infections and inflammatory diseases through activation of the JAK-STAT5 pathway.[44 45] Our study revealed that, compared with $CD4^+GzmB^+$ T cells, $CD4^+GzmB^+$ T cells expressed CD57 but lost CD28, which is a phenotype similar to that of the cytotoxic $CD4^+$ T cells identified in chronic inflammatory diseases. We demonstrated that IL-15-mediated STAT5 signaling was responsible for increasing the proliferative capability of $CD4^+GzmB^+$ T cells but did not affect T-bet expression. The combination of IL-15 and anti-CD3/CD28 antibodies induced the activation of AKT, and subsequently, the cytoplasmic sequestration of FOXO1 by AKT-mediated phosphorylation of FOXO1 was responsible for T-bet and GzmB upregulation in $CD4^+$ T cells. Nevertheless, our results indicate that in the context of various diseases, cytotoxic $CD4^+$ T cells may have a common characteristic, which is the requirement for IL-15-mediated signaling to promote the activation of these cells.

It is well recognized that T-bet, Eomes, and Runx3 are required for the differentiation of effector cytolytic $CD8^+$ T cells.[14] In our study, we found that IL-5 differentially regulated T-bet and Eomes expression in $CD4^+GzmB^+$ T cells. IL-15-stimulated PBMCs or TILs increased T-bet expression while reducing Eomes expression in $CD4^+GzmB^+$ T cells. In addition to playing key roles in the generation of cytotoxic T cells, T-bet and Eomes are also essential players in determining whether activated $CD8^+$ T cells become memory precursors or short-lived effector cells, although the underlying mechanism remains unclear.[46 47] Moreover, T-bet and Eomes also control the process of generating effector or exhausted T cells.[48 49] Given the complex roles of Eomes in T cells, the discrepancy in the effects of Eomes on $CD4^+GzmB^+$ T cells could be explained by the fact that some $CD4^+GzmB^+$ T cells in PBMCs and TILs expressed high levels of Eomes and exhibited a memory or exhaustion phenotype. IL-15 stimulation resulted in the downregulation of Eomes in $CD4^+GzmB^+$ T cells, which might indicate that IL-15 restores the effector function of these cells. Further studies with more in-depth analyses to verify the role of the IL-15-induced downregulation of Eomes in restoring intratumoral $CD4^+GzmB^+$ T-cell functions are needed.

Interestingly, SLC7A5 expression was higher in $CD4^+GzmB^+$ T cells ex vivo than in their counterparts, which has not been previously reported. SLC7A5 is an amino acid transporter that is upregulated by TCR stimulation, which in turn activates T cells through an influx of amino acids.[32] SLC7A5-null T cells fail to undergo clonal expansion and effector differentiation in response to antigens.[50] A very recent study reported that blocking SLC7A5 with JPH203 did not affect the production of IL-2 by $CD4^+$ naïve T cells, whereas IL-17A and IFN-γ production by $CD4^+$ memory T cells was greatly reduced.[51] Our study showed for the first time that IL-15 signaling facilitates the effector functions of $CD4^+GzmB^+$ T cells via an increase in SLC7A5 expression in these cells. Low doses of JPH203 inhibited GzmB expression but not IFN-γ expression, further confirming that SLC7A5 plays an essential role in $CD4^+GzmB^+$ T-cell development. SLC7A5 was shown to be involved in increasing T-bet and GzmB expression in $CD4^+$ CTLs via activation of mTORC1.

In this study, we also revealed that dual blockade of PD-1 and CD85j facilitated the cytolytic activity of $CD4^+GzmB^+$ T cells. CD85j (also known as ILT2), an inhibitory receptor that binds the non-classic MHC-I HLA-molecule HLA-G, is expressed in immune cells, including subsets of T cells.[52] A recent study revealed that in patients with clear cell renal cell carcinoma, tumor-infiltrating and peripheral $CD4^+CD85j^+$ T cells exhibited cytolytic activity and were selectively inhibited by HLA-G expressed on cancer cells.[53] Our results were in line with these findings, as we showed that $CD4^+GzmB^+$ T cells expressed higher levels of CD85j than did $CD4^+GzmB^-$ T cells. Moreover, blockade of CD85j increased the number of intratumoral $CD4^+GzmB^+$ T cells but did not affect the proportion of $CD8^+GzmB^+$ T cells because of the unique expression pattern of CD85j in these cells. More importantly, we showed for the first time that in patients with NSCLC, tumor-infiltrating $CD4^+GzmB^+$ T cells exclusively expressed either PD-1 or CD85j; therefore, in the PDE model, dual blockade of PD-1 and CD85j significantly increased the number of $CD4^+GzmB^+$ T cells and Ki67 expression in this subset of cells. Our study provides a strong rationale for dual blockade therapy aimed at enhancing the efficacy of $CD4^+GzmB^+$ T-cell-mediated antitumor immunity.

In the PDE model, we observed a strong association between the expression level of MHC-II in tumor cells and the responsiveness of $CD4^+GzmB^+$ T cells to immunotherapy. Accumulating evidence has demonstrated that tumor-specific MHC-II is associated with favorable prognosis in patients with cancer, including those

treated with immunotherapies.[54] Johnson *et al*, using immunocompetent murine models of NSCLC, demonstrated that cancer cell-intrinsic MHC-II correlated with the response to anti-PD-1 therapy.[55] Our in vitro study demonstrated that MHC-II expression in tumor cells was required for $CD4^+GzmB^+$ T cells to directly kill these cells. Additionally, in vivo experiments revealed that the use of a gain-of-function approach to overexpress CIITA in LLC cells resulted in an increase in the number of intratumoral $CD4^+GzmB^+$ T cells, leading to a significant improvement in the tumor response to anti-PD-1 therapy compared with MHC-II-negative LLC tumors. Notably, we did not find a clear association between HLA-DR expression in tumor cells and the proportion of intratumoral $CD4^+GzmB^+$ T cells among total $CD4^+$ T cells ex vivo. These results suggest that MHC-II expression in tumor cells might not be required for the differentiation of $CD4^+GzmB^+$ T cells but is essential for fully restoring the effector function of intratumoral $CD4^+GzmB^+$ T cells.

Thus, this study provides new insights into the molecular mechanisms underlying the differentiation of $CD4^+GzmB^+$ T cells and identifies the critical factors that drive $CD4^+GzmB^+$ T-cell transformation in the tumor microenvironment of MCH-II-expressing tumors.

Acknowledgements We thank the Medical Subcenter of HUST Analytical and Testing Center and Experimental Medicine Center, Tongji Hospital, Tongji Medical College, Huazhong University of Science and Technology, for data acquisition.

Contributors Conceptualization: BW, XF and LL. Methodology: BW, Xu Wang, TW, KM, TY, ZY and RQ. Investigation: YX, SH and HX. Visualization: WZ, YT and CZ. Funding acquisition: XF and LL. Project administration: YC, SF and XF. Supervision: XF and LL. Writing original draft: BW and LL. Writing review and editing: BW, Xu Wang, TW, YX, KM, YT, Xue Wang and LL. All authors read and approved of the manuscript. The guarantor for the study is LL.

Funding This work was supported by the National Natural Science Foundation of China (grant numbers: 82473303, 82173103 and 81874168 to LL, 82473302 to XF) and Research Funds by the Department of Finance of Hubei Province (SCZ202104 and SCZ202201 to XF).

Competing interests No, there are no competing interests.

Patient consent for publication Not applicable.

Ethics approval This study was approved by the Huazhong University of Science and Technology Ethics Committee (ID: 20240367). All Participants gave informed consent to participate in the study before taking part. Besides, all experimental procedures involving mice were also conducted in accordance with the Huazhong University of Science and Technology Ethics Committee (ID: 202210027).

Provenance and peer review Not commissioned; externally peer reviewed.

Data availability statement Data are available on reasonable request. RNA-seq data for this study were deposited in the Gene Expression Omnibus (GEO) under the GSE277852 dataset.

ORCID iDs
Boyu Wang http://orcid.org/0009-0003-9284-9852
Zhiwei Yuan http://orcid.org/0000-0002-6426-9573
Lequn Li http://orcid.org/0000-0002-6582-142X

REFERENCES

1 Raskov H, Orhan A, Christensen JP, *et al*. Cytotoxic CD8(+) T cells in cancer and cancer immunotherapy. *Br J Cancer* 2021;124:359–67.
2 van der Leun AM, Thommen DS, Schumacher TN. CD8(+) T cell states in human cancer: insights from single-cell analysis. *Nat Rev Cancer* 2020;20:218–32.
3 Tay RE, Richardson EK, Toh HC. Revisiting the role of CD4(+) T cells in cancer immunotherapy-new insights into old paradigms. *Cancer Gene Ther* 2021;28:5–17.
4 Guo M, Liu MYR, Brooks DG. Regulation and impact of tumor-specific CD4(+) T cells in cancer and immunotherapy. *Trends Immunol* 2024;45:303–13.
5 Oh DY, Kwek SS, Raju SS, *et al*. Intratumoral CD4(+) T Cells Mediate Anti-tumor Cytotoxicity in Human Bladder Cancer. *Cell* 2020;181:1612–25.
6 Lin W, Singh V, Springer R, *et al*. Human CD4 cytotoxic T lymphocytes mediate potent tumor control in humanized immune system mice. *Commun Biol* 2023;6:447.
7 Bawden EG, Wagner T, Schröder J, *et al*. CD4(+) T cell immunity against cutaneous melanoma encompasses multifaceted MHC II-dependent responses. *Sci Immunol* 2024;9:eadi9517.
8 Mucida D, Husain MM, Muroi S, *et al*. helper T cells generates distinct MHC class II-restricted cytotoxic T lymphocytes. *Nat Immunol* 2013;14:281–9.
9 Yang X, Wu J, Fan L, *et al*. Single-Cell Analysis Identifies Distinct Populations of Cytotoxic CD4(+) T Cells Linked to the Therapeutic Efficacy of Immune Checkpoint Inhibitors in Metastatic Renal Cell Carcinoma. *J Inflamm Res* 2024;17:4505–23.
10 Hashimoto K, Kouno T, Ikawa T, *et al*. Single-cell transcriptomics reveals expansion of cytotoxic CD4 T cells in supercentenarians. *Proc Natl Acad Sci U S A* 2019;116:24242–51.
11 Hong X, Meng S, Tang D, *et al*. Single-Cell RNA Sequencing Reveals the Expansion of Cytotoxic CD4(+) T Lymphocytes and a Landscape of Immune Cells in Primary Sjögren's Syndrome. *Front Immunol* 2020;11:594658.
12 Wang B, Hu S, Fu X, *et al*. CD4(+) Cytotoxic T Lymphocytes in Cancer Immunity and Immunotherapy. *Adv Biol* 2023;7:e2200169.
13 Takeuchi A, Saito T. CD4 CTL, a Cytotoxic Subset of CD4(+) T Cells, Their Differentiation and Function. *Front Immunol* 2017;8:194.
14 Cruz-Guilloty F, Pipkin ME, Djuretic IM, *et al*. Runx3 and T-box proteins cooperate to establish the transcriptional program of effector CTLs. *J Exp Med* 2009;206:51–9.
15 Knudson CJ, Férez M, Alves-Peixoto P, *et al*. Mechanisms of Antiviral Cytotoxic CD4 T Cell Differentiation. *J Virol* 2021;95:e00566-21.
16 Taniuchi I. CD4 Helper and CD8 Cytotoxic T Cell Differentiation. *Annu Rev Immunol* 2018;36:579–601.
17 Ye F, Cai Z, Wang B, *et al*. TGFβ Antagonizes IFNγ-Mediated Adaptive Immune Evasion via Activation of the AKT-Smad3-SHP1 Axis in Lung Adenocarcinoma. *Cancer Res* 2023;83:2262–77.
18 Yamada H, Kaibara N, Okano S, *et al*. Interleukin-15 selectively expands CD57+ CD28- CD4+ T cells, which are increased in active rheumatoid arthritis. *Clin Immunol* 2007;124:328–35.
19 Chen B, Morris SR, Panigrahi S, *et al*. Cytomegalovirus Coinfection Is Associated with Increased Vascular-Homing $CD57^+$ CD4 T Cells in HIV Infection. *J Immunol* 2020;204:2722–33.
20 Ozdemir O, Savaşan S. Combinational IL-2/IL-15 induction does not further enhance IL-15-induced lymphokine-activated killer cell cytotoxicity against human leukemia/lymphoma cells. *Clin Immunol* 2005;115:240–9.
21 Cheuk S, Schlums H, Gallais Sérézal I, *et al*. CD49a Expression Defines Tissue-Resident CD8(+) T Cells Poised for Cytotoxic Function in Human Skin. *Immunity* 2017;46:287–300.
22 Huang B, Liu R, Wang P, *et al*. CD8(+)CD57(+) T cells exhibit distinct features in human non-small cell lung cancer. *J Immunother Cancer* 2020;8.
23 Hu S, Meng K, Wang T, *et al*. Lung cancer cell-intrinsic IL-15 promotes cell migration and sensitizes murine lung tumors to anti-PD-L1 therapy. *Biomark Res* 2024;12:40.

24 Katsuyama E, Suarez-Fueyo A, Bradley SJ, *et al*. The CD38/NAD/SIRTUIN1/EZH2 Axis Mitigates Cytotoxic CD8 T Cell Function and Identifies Patients with SLE Prone to Infections. *Cell Rep* 2020;30:112–23.
25 Pradier A, Simonetta F, Waldvogel S, *et al*. Modulation of T-bet and Eomes during Maturation of Peripheral Blood NK Cells Does Not Depend on Licensing/Educating KIR. *Front Immunol* 2016;7:299.
26 Shan Q, Zeng Z, Xing S, *et al*. The transcription factor Runx3 guards cytotoxic CD8(+) effector T cells against deviation towards follicular helper T cell lineage. *Nat Immunol* 2017;18:931–9.
27 Reis BS, Hoytema van Konijnenburg DP, Grivennikov SI, *et al*. Transcription factor T-bet regulates intraepithelial lymphocyte functional maturation. *Immunity* 2014;41:244–56.
28 Rao RR, Li Q, Gubbels Bupp MR, *et al*. Transcription factor Foxo1 represses T-bet-mediated effector functions and promotes memory CD8(+) T cell differentiation. *Immunity* 2012;36:374–87.
29 Shehata HM, Khan S, Chen E, *et al*. Lack of Sprouty 1 and 2 enhances survival of effector CD8(+) T cells and yields more protective memory cells. *Proc Natl Acad Sci U S A* 2018;115:E8939–47.
30 Lückel C, Picard F, Raifer H, *et al*. IL-17(+) CD8(+) T cell suppression by dimethyl fumarate associates with clinical response in multiple sclerosis. *Nat Commun* 2019;10:5722.
31 Ren W, Liu G, Yin J, *et al*. Amino-acid transporters in T-cell activation and differentiation. *Cell Death Dis* 2017;8:e2655.
32 Wang W, Zou W. Amino Acids and Their Transporters in T Cell Immunity and Cancer Therapy. *Mol Cell* 2020;80:384–95.
33 Ni M, Yue Z, Tian M, *et al*. Leucine-Mediated *SLC7A5* Promotes Milk Protein and Milk Fat Synthesis through mTOR Signaling Pathway in Goat Mammary Epithelial Cells. *J Agric Food Chem* 2024;72:13728–39.
34 Lv Y, Li M, Weng L, *et al*. Ginseng-derived nanoparticles reprogram macrophages to regulate arginase-1 release for ameliorating T cell exhaustion in tumor microenvironment. *J Exp Clin Cancer Res* 2023;42:322.
35 Morel E, Bellón T. Amoxicillin conjugates to HLA class I molecules and interferes with signalling through the ILT2/LIR-1/CD85j inhibitory receptor. *Allergy* 2007;62:190–6.
36 Borgeaud M, Sandoval J, Obeid M, *et al*. Novel targets for immune-checkpoint inhibition in cancer. *Cancer Treat Rev* 2023;120:102614.
37 Qin S, Xu L, Yi M, *et al*. Novel immune checkpoint targets: moving beyond PD-1 and CTLA-4. *Mol Cancer* 2019;18:155.
38 Toor SM, Murshed K, Al-Dhaheri M, *et al*. Immune Checkpoints in Circulating and Tumor-Infiltrating CD4$^+$ T Cell Subsets in Colorectal Cancer Patients. *Front Immunol* 2019;10:2936.
39 Shekarian T, Zinner CP, Bartoszek EM, *et al*. Immunotherapy of glioblastoma explants induces interferon-γ responses and spatial immune cell rearrangements in tumor center, but not periphery. *Sci Adv* 2022;8:eabn9440.
40 Yang Y, Sun J, Wang Z, *et al*. Updated Overall Survival Data and Predictive Biomarkers of Sintilimab Plus Pemetrexed and Platinum as First-Line Treatment for Locally Advanced or Metastatic Nonsquamous NSCLC in the Phase 3 ORIENT-11 Study. *J Thorac Oncol* 2021;16:2109–20.
41 Chu X, Tian W, Wang Z, *et al*. Co-inhibition of TIGIT and PD-1/PD-L1 in Cancer Immunotherapy: Mechanisms and Clinical Trials. *Mol Cancer* 2023;22:93.
42 Naji A, Menier C, Maki G, *et al*. Neoplastic B-cell growth is impaired by HLA-G/ILT2 interaction. *Leukemia* 2012;26:1889–92.
43 Riley JL. PD-1 signaling in primary T cells. *Immunol Rev* 2009;229:114–25.
44 Zhang T, Liu X, Zhao Y, *et al*. Excessive IL-15 promotes cytotoxic CD4(+)CD28- T cell-mediated renal injury in lupus nephritis. *Immun Ageing* 2022;19:50.
45 Wang T, Wei L, Meng S, *et al*. Coordinated Priming of NKG2D Pathway by IL-15 Enhanced Functional Properties of Cytotoxic CD4$^+$CD28$^-$T Cells Expanded in Systemic Lupus Erythematosus. *Inflammation* 2023;46:1587–601.
46 Hamilton SE, Jameson SC. CD8(+) T cell differentiation: choosing a path through T-bet. *Immunity* 2007;27:180–2.
47 Seo W, Jerin C, Nishikawa H. Transcriptional regulatory network for the establishment of CD8(+) T cell exhaustion. *Exp Mol Med* 2021;53:202–9.
48 Wherry EJ. T cell exhaustion. *Nat Immunol* 2011;12:492–9.
49 Paley MA, Kroy DC, Odorizzi PM, *et al*. Progenitor and terminal subsets of CD8(+) T cells cooperate to contain chronic viral infection. *Science* 2012;338:1220–5.
50 Sinclair LV, Rolf J, Emslie E, *et al*. Control of amino-acid transport by antigen receptors coordinates the metabolic reprogramming essential for T cell differentiation. *Nat Immunol* 2013;14:500–8.
51 Kang YJ, Song W, Lee SJ, *et al*. Inhibition of BCAT1-mediated cytosolic leucine metabolism regulates Th17 responses via the mTORC1-HIF1α pathway. *Exp Mol Med* 2024;56:1776–90.
52 Gustafson CE, Qi Q, Hutter-Saunders J, *et al*. Immune Checkpoint Function of CD85j in CD8 T Cell Differentiation and Aging. *Front Immunol* 2017;8:692.
53 Jacquier A, Lambert T, Delattre J-F, *et al*. Tumor infiltrating and peripheral CD4(+)ILT2(+) T cells are a cytotoxic subset selectively inhibited by HLA-G in clear cell renal cell carcinoma patients. *Cancer Lett* 2021;519:105–16.
54 Axelrod ML, Cook RS, Johnson DB, *et al*. Biological Consequences of MHC-II Expression by Tumor Cells in Cancer. *Clin Cancer Res* 2019;25:2392–402.
55 Johnson AM, Bullock BL, Neuwelt AJ, *et al*. Cancer Cell-Intrinsic Expression of MHC Class II Regulates the Immune Microenvironment and Response to Anti-PD-1 Therapy in Lung Adenocarcinoma. *J Immunol* 2020;204:2295–307.